Original articles

Inhibitors of chloride corrosion of reinforcement steel in concrete based on derivatives of salts of carboxylic acids and dimethylaminopropylamine

O. A. Kozaderov✉, D. S. Shevtsov, M. A. Potapov, I. D. Zartsyn, S. N. Grushevskaya,
A. A. Kruzhilin, E. A. Ilina, K. A. Tkachenko, Kh. S. Shikhaliev

Voronezh State University,
1 Universitetskaya pl., Voronezh 394018, Russian Federation

Abstract

In our study, we synthesised derivatives of salts of carboxylic acids and dimethylaminopropylamine: 3-(dimethylamino) propyl-1-ammonium acetate, 3-(dimethylamino)propyl-1-ammonium hexanoate, 3-(dimethylamino)propyl-1-ammonium octanoate, and 3-(dimethylamino)propyl-1-ammonium terephthalate. The structures of the molecules of the obtained substances were confirmed using physical methods: Fourier-transform infrared spectroscopy, NMR spectroscopy, and HPLC.

Electrochemical methods (voltammetry and electrochemical impedance spectroscopy) and quantum chemical modeling were used to assess the inhibitory effect of the synthesised substances with regard to 35GS reinforcement steel. Experiments were conducted in a water extract from a mortar simulating concrete pore solution in the presence of chlorides inducing pitting corrosion. 3-(dimethylamino)propyl-1-ammonium terephthalate is expected to have the highest degree of protection (up to 71%) at a concentration of 2.0 g·dm^{-3}. The highest degree of protection for the derivatives with alkyl radicals is 41–46% in a range of concentrations from 0.5 to 2.0 g·dm^{-3}. The results of potentiodynamic measurements and quantum chemical modeling were close. Average level of degree of protection can be explained by a high concentration of chlorides in the model solution (1.00 mol·dm^{-3}). The effectiveness of the obtained substances is to be further studied using fine-grained concrete. This will help to assess the impact of the additives on the capillary pore structure (permeability) of concrete and the concentration of chlorides.

Keywords: Reinforcement steel, Reinforced concrete, Corrosion inhibitors, Chlorides, Dimethylaminopropylamine derivatives

For citation: Kozaderov O. A., Shevtsov D. S., Potapov M. A., Zartsyn I. D., Grushevskaya S. N., Kruzhilin A. A., Ilina E. A., Tkachenko K. A., Shikhaliev Kh. S. Inhibitors of chloride corrosion of reinforcement steel in concrete based on derivatives of salts of carboxylic acids and dimethylaminopropylamine. *Condensed Matter and Interphases*. 2023;25(3): 435–444 . https:// doi.org/10.17308/kcmf.2023.25/11393

Для цитирования: Козадеров О. А., Шевцов Д. С., Потапов М. А., Зарцын И. Д., Грушевская С. Н., Кружилин А. А., Ильина Е. А., Ткаченко К. А., Шихалиев Х. С. Ингибиторы хлоридной коррозии арматурной стали в бетоне на основе производных солей карбоновых кислот и диметиламинопропиламина. *Конденсированные среды и межфазные границы*. 2023;25(3): 435–444. https://doi.org/10.17308/kcmf.2023.25/11393

✉ Oleg A. Kozaderov, e-mail: ok@chem.vsu.ru

Condensed Matter and Interphases / Конденсированные среды и межфазные границы   2023;25(3): 435–444

O. A. Kozaderov et al.   Inhibitors of chloride corrosion of reinforcement steel in concrete...

1. Introduction

The design life of reinforced concrete structures should be at least 50–100 years depending on the area of application and design features [1]. This parameter can decrease significantly during operation, especially in highly corrosive environments. As a result, the first signs of distress appear during the early stages of operation [2]. Preventive maintenance and capital repairs using specialized fine-grained concrete are common practice [3]. However, this approach is often hard to implement. For instance, due to the continuity of the production process it is impossible to stop the operation of a certain structure without shutting down the whole production line. Considering the fact that large enterprises endure enormous financial losses because of long downtime, which exceed the cost of repair several times [4], it is important to make reinforced concrete structures as durable as possible.

The main cause of degradation of reinforced concrete structures is corrosion of reinforcement bars, with the contribution of processes induced by chlorides being over 65% [5]. Therefore, the structures most susceptible to chloride corrosion are those located on the coast, as well as transport infrastructure facilities and motorways coated with antifreeze reagents, chemical industry facilities producing mineral fertilizers, etc. Primary and secondary protection of reinforced concrete is used to prevent corrosion [6]. At the same time coatings, surface treatment, and other secondary protection methods require additional time and expenses [7]. Although secondary protection is the only way to ensure the required durability in certain environments (e.g. aggressive acids) [8], primary protection measures, i.e. finding the optimal composition of concrete, are generally the easiest to implement.

To increase the corrosion resistance of steel reinforcement bars in concrete, various additives reducing the permeability of concrete [9, 10] or corrosion inhibitors [11, 12] are used, which can reduce the rate of corrosion of steel and affect the physical and mechanical properties of concrete at the same time. To reduce the time of analysis of their effect, model liquid solutions are used: a saturated solution of $Ca(OH)_2$ [13–16], its modifications whose compositions are close to the actual composition of the concrete pore solution,

and extracts obtained from cement and ground concrete [17, 18]. The concentration of chlorides (C_{Cl}) introduced to induce corrosion varies from 0.1 to 0.9 mol·dm^{-3} (5% wt.). This parameter affects the degree of protection: the higher the concentration of chlorides, the lower the protection degree.

We should note that experiments with model aqueous electrolyte solutions demonstrate only the true inhibitory effect of the studied substance on steel reinforcement. When used in actual concretes, the protective effect can be significantly greater due to the compaction of concrete (the plastification effect) or lower (due to increased permeability, air entrainment, etc.).

Therefore, it is important to determine the most effective inhibitors of corrosion of steel reinforcement in concrete affected by chlorides. At the moment, a large number of inorganic (nitrites, chromates, phosphates, etc. [16–18]), organic (amines and carboxylic acids [13, 19, 20], triazoles [21], salts of benzoic acid [22], hydroquinoline and pyrocatechol [23], siloxanes [24], etc.), natural compounds [25, 26], and compositions based on them [27–29] are being studied. Due to the great protective effect of carboxylic acids, including long-chain carboxylic acids, against corrosion of steel reinforcement bars in concrete, it is of great scientific and practical importance to study the inhibitory properties of their derivatives.

The purpose of our study was to synthesize and assess the inhibitory properties of new derivatives of salts of carboxylic acids and dimethylaminopropylamine with regard to low-carbon reinforcement steel in an aqueous solution simulating a concrete environment in the presence of chlorides.

2. Experimental

2.1. Synthesis and analysis of dimethylaminopropylamine derivatives

In our study, we obtained a series of ammonium salts of dimethylaminopropylamine with certain carboxylic acids (Table 1) with different lengths of the hydrocarbon radicals as potential inhibitors of chloride corrosion of steel reinforcement bars in reinforced concrete. All reagents used were purchased from Acros Organics.

The inhibitors were synthesised as follows: a mixture of 1 mol of acid, 1 mol of amine (2 mol for **d**), and 50 ml of ethanol was boiled until

Condensed Matter and Interphases / Конденсированные среды и межфазные границы   2023;25(3): 435–444

O. A. Kozaderov et al.   Inhibitors of chloride corrosion of reinforcement steel in concrete…

all the components dispersed completely. The completeness of the reaction was controlled using a universal indicator and thin-layer chromatography. After the neutralization, the obtained homogeneous solution was evaporated on a rotary evaporator until the solvent evaporated. The scheme of the process is presented below.

D

A-C

R: CH₃, C₅H₁₁, C₇H₁₅
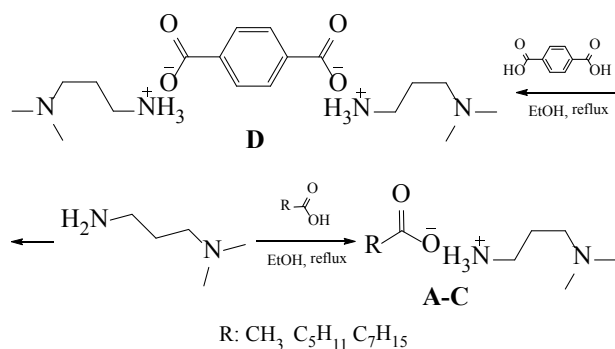
The obtained ammonium salts were analysed using high-performance liquid chromatography with high-resolution mass spectrometry (electrospray ionization, HPLC-HRMS-ESI) in combination with UV detection. The analyser unit included an Agilent 1269 Infinity chromatograph and an Agilent 6230 TOF LC/MS detector. Quantitative analysis was performed using an external standard method. 1H NMR spectra were recorded using a Bruker AV600 (600, 13 MHz) spectrometer in a DMSO-d6. TMS was used as the internal standard. The IR spectrum was recorded on Vertex 70 FT-IR spectrometer using a Platinum ATR (Bruker) ATR attachment equipped with a diamond prism in the frequency range from 4000 to 400 cm⁻¹ with a resolution of 2 cm⁻¹. The result was obtained by averaging 16 scans.

The study demonstrated that in the absence of a catalyst, when equimolar amounts of dimethylaminopropylamine and carboxylic acids are boiled in ethanol, a neutralization reaction takes place with almost quantitative yields of the corresponding ammonium salts. This is confirmed by LC/MS spectrometry, 1H NMR spectrometry, and IR spectrometry.

3-(dimethylamino)propyl-1-ammonium acetate (**a**). 95% yield, amber viscous liquid. 1H NMR (δ): 1.84–1.91 (m, 2H 1CH₂), 2.22 (s, 3H CH₃), 2.37–2.41 (s, 6H 2CH₃), 2.60–2.67 (m, 2H 1CH₂), 2.90–2.97 (*m*, 2H 1CH₂). IR spectrum (cm⁻¹): 3300–3400 (OH + N⁺-H), 2150–2200 (N⁺-H), 1700–1750 (C=O), 1550–1600 (COO⁻ + C-O-H), 1550 (N⁺H), 1400 (N⁺H), 900–1150 (CH₂), 750–800 (CH₂). Determined, *m/z*: 163.1162 [M+H]⁺. Calculated, *m/z* 163.1368 [M+H]⁺.

3-(dimethylamino)propyl-1-ammonium hexanoate (**b**). 96% yield, amber viscous liquid. 1H NMR (δ): 0.89–0.90 (*t*, 3H CH₃), 1.20–1.23 (*m*, 6H 3CH₂), 1.85–1.90 (m, 2H 1CH₂), 2.35–2.43 (s, 8H 2CH₃+βCH₂), 2.61–2.65 (m, 2H 1CH₂), 2.91–2.92 (*m*, 2H 1CH₂). IR spectrum (cm⁻¹): 3300–3400 (OH + N⁺-H), 2150–2200 (N⁺-H), 1700–1750 (C=O), 1550–1600 (COO⁻ + C-O-H), 1550 (N⁺H), 1400 (N⁺H), 900–1150 (CH₂), 750–800 (CH₂). Determined, *m/z*: 218.1862 [M+H]⁺. Calculated, m/z: 218.1994 [M+H]⁺.

Table 1. Studied inhibitors

Symbol	Name	Formula
a	3-(dimethylamino)propyl-1-ammonium acetate	
b	3-(dimethylamino)propyl-1-ammonium hexanoate	
c	3-(dimethylamino)propyl-1-ammonium octanoate	
d	3-(dimethylamino)propyl-1-ammonium terephthalate	

Condensed Matter and Interphases / Конденсированные среды и межфазные границы 2023;25(3): 435–444

O. A. Kozaderov et al. Inhibitors of chloride corrosion of reinforcement steel in concrete...

3-(dimethylamino)propyl-1-ammonium octanoate **(c)**. 94% yield, amber viscous liquid. 1H NMR (δ): 0.87–0.91 (*t*, 3H CH$_3$), 1.19–1.86 (*m*, 14H 5CH$_2$+βCH$_2$+CH$_2$), 2.25–2.33 (s, 6H 2CH$_3$), 2.60–2.63 (m, 2H CH$_2$), 2.92–2.94 (*m*, 2H CH$_2$). IR spectrum (cm^{-1}): 3300–3400 (OH + N$^+$-H), 2150–2200 (N$^+$-H), 1700–1750 (C=O), 1550–1600 (COO$^-$ + C-O-H), 1550 (N$^+$H), 1400 (N$^+$H), 900–1150 (CH$_2$), 750–800 (CH$_2$), Determined, *m/z*: 246.3154 [M+H]$^+$. Calculated, m/z: 246.2307 [M+H]$^+$.

3-(dimethylamino)propyl-1-ammonium terephthalate **(d)**. 85% yield, white crystalline substance, mp = 273–275 °C. 1H NMR (δ): 1.84–1.91 (m, 4H 2CH$_2$), 2.41–2.45 (m, 12H 6CH$_3$), 2.64–2.71 (m, 4H 2CH$_3$), 2.90–2.97 (*m*, 4H 2CH$_2$), 7.92 (d, 4H, aromatic). IR spectrum (cm^{-1}): 3300–3400 (OH + N$^+$-H), 2150–2200 (N$^+$-H), 1550–1600 (COO$^-$ + C-O-H), 1550 (N$^+$H), 1400 (N$^+$H), 900–1150 (CH$_2$), 750–800 (CH$_2$), 500–600 (C-H aromatic). Determined, *m/z*: 370.1290 [M+H]$^+$. Calculated, m/z: 370.2580 [M+H]$^+$.

2.2. Assessment of the corrosion inhibition properties

To evaluate the corrosion inhibition properties of the synthesised compounds, a set of electrochemical methods was used. Quantum-chemical calculations were also performed.

Samples of low-carbon 35GS steel with rectangular section were used as the working electrode. All the surfaces, except for the working surface, were mounted in epoxy resin. Saturated silver chloride reference electrode (SCE, +201 mV relative to the standard hydrogen electrode) was placed in a separate container linked to the electrolytic cell by an agar-agar based salt bridge filled with a KNO$_3$ saturated solution. The potentials in the study are presented relative to the standard hydrogen electrode. A platinum grid was used as an auxiliary electrode.

The working solution was a water extract from cement powder (mass ratio of distilled water and cement powder 1:10, extraction for 24 hours followed by filtration, pH 12.5–13.0). Electrochemical measurements were conducted in a glass three-electrode cell with undivided electrode spaces at a temperature of 23±3 °C under natural aeration conditions, in the presence of the inhibitor NaCl with the concentration of

1.00 mol·dm^{-3} (reference experiment) and the studied substances.

The working electrode was preliminarily cleaned with K2000 sandpaper, washed with distilled water, and degreased with chemically pure isopropyl alcohol. The current density *i* was calculated by dividing the actual current *I* by the geometric area of the working electrode (2.25 cm^2).

The corrosion current density (i_{cor}) was determined by the polarization resistance (PR) technique as summarized by Mansfeld [30]. After the free corrosion potential (E_{cor}) became stable, the polarization curve was registered for 30 minutes using an IPC-Pro potentiostat in the potentiodynamic polarization mode (potential scan rate of 0.2 mV·s^{-1}) in the range from E_{cor} −30 mV to E_{cor}+30 mV.

The ability of the studied substances to inhibit corrosion was assessed based on the degree of protection calculated using the formula:

$$Z_i = \frac{i_{cor,0} - i_{cor,inh}}{i_{cor,0}} \cdot 100\,\%,$$

where $i_{cor,0}$ and $i_{cor,inh}$ are the corrosion current density during the reference experiment and in the presence of the inhibitor respectively.

The electrochemical impedance spectroscopy (EIS) was performed using the IPC-Pro potentiostat with a frequency response analyser FRA-2. After E_{corr} was stable for 30 minutes, the frequency dependent impedance was registered within the range from 0.01 to 50 Hz with no current. The analysis of frequency dependences, the selection of the equivalent circuit, and determining its component values was carried out using DCS software. The results are presented as a Nyquist diagram. The inhibition efficiency (η_{inh}) was calculated using the formula:

$$\eta_{inh} = \left(1 - \frac{R_{p,0}}{R_{p,inh}}\right) \cdot 100,$$

where $R_{p,0}$ and $R_{p,inh}$ are polarization resistance in the reference experiment and in the presence of the inhibitor respectively.

The optimisation of the geometry of the studied inhibitor molecules was carried out within the framework of the density functional theory (DFT) using the B3LYP functional

Condensed Matter and Interphases / Конденсированные среды и межфазные границы   2023;25(3): 435–444

O. A. Kozaderov et al.   Inhibitors of chloride corrosion of reinforcement steel in concrete...

with basis 6-311+ G(d,p) in the Gaussian 09 package. The optimized geometry of molecules is characterized by a lack of negative oscillation frequencies and therefore corresponds to the minimum value on the potential energy surface. In addition, TDDFT (time-dependent density functional theory) calculations for optimized geometry were performed to find the five lowest electronic excitations. Energies of HOMO and LUMO molecular orbitals were used to forecast the inhibition effectiveness. Within the limitation of the Koopmans' theorem, the energies of frontier orbitals are determined by the formulas:

$$-E_{HOMO} = IP \text{ and } -E_{LUMO} = EA.$$

Here IP is ionisation potential, and EA is electron affinity. The inhibition effectiveness was assessed based on the chemical hardness:

$$\eta = \frac{IP - EA}{2}$$

and softness:

$$\sigma = \frac{1}{\eta}.$$

3. Results and discussion

3.1. Potentiodynamic measurements

Substance **a** does not have any significant effect on the free corrosion potential of low-carbon steel in the presence of chlorides in the whole range of concentrations studied (taking into account the accuracy of measurements) (Table 2).

When substances **b-d** were introduced, E_{cor} shifted towards positive values by 35–80 mV, which indicates the effect primarily on the partial anodic oxidation of metal [31]. This is also confirmed by the comparison of the initial sections of the polarization curves. Thus, for **a, b** cathodic sections of the polarization curves for all concentrations of the inhibitor C_{inh} practically coincide with the reference. Anodic sections, when $C_{inh} \geqslant 1.0$ g·dm^{-3}, demonstrated monotonous reduction of the current density at a given value of the electrode potential (Fig. 1a). For **b,** monotonous reduction in i on the anodic sections of the polarization curve was registered at $C_{inh} \geqslant 0.5$ g·dm^{-3} (Fig. 1b).

The introduction of **c** reduced the current density on both cathodic and anodic section of the polarization curve as compared to the reference experiment (Fig. 1c). When the concentration of chlorides was $C_{inh} = 0.5$ and 1.0 g·dm^{-3} cathodic sections were not registered, while the current density on the anodic sections was lower at $C_{inh} = 0.5$ g·dm^{-3}. The lowest values of i were obtained when $C_{inh} = 2.0$ g·dm^{-3}.

For **d** at higher C_{inh} the anodic current density decreased monotonously, while the cathodic section of the polarization curve decreased only when $C_{inh} = 1.0$ g·dm^{-3}.

The calculations of the electrochemical parameters by means of polarization resistance technique are given in Table 2. They are compatible with the results of the analysis of the polarization curves. The protection degree generally increases at higher concentrations of the substance (except for **c**). For **a-c** Z_i reaches 41–

Table 2. Kinetic parameters of mild steel electrode in water extract from cement + 1.00 mol·dm^{-3} NaCl in the presence of derivatives of dimethylaminopropylamine

Inhibitor	C_{inh}, g·dm^{-3}	E_{cor}, mV	R_p, kΩ·cm^2	b_a, mV	b_c, mV	B, mV	i_{cor}, μA·cm^{-2}	Z_i, %
blank	–	−451	9.21	64.3	63.0	31.8	3.44±0.36	–
a	0.5	−439	8.49	59.9	59.9	30.0	3.52±0.28	−2
	1.0	−453	10.56	53.4	40.4	23.0	2.20±0.30	36
	2.0	−458	10.97	50.4	35.2	20.7	1.92±0.25	44
b	0.5	−414	9.60	65.6	38.2	24.2	2.54±0.28	26
	1.0	−410	11.80	64.7	33.9	22.3	1.87±0.13	46
c	0.5	−374	13.27	65.6	46.5	27.2	2.05±0.19	41
	1.0	−370	12.03	78.2	55.1	32.4	2.71±0.22	21
	2.0	−401	14.08	86.4	49.5	31.5	2.22±0.10	36
d	0.5	−398	12.13	51.2	35.2	20.9	1.73±0.21	50
	1.0	−405	17.44	46.0	27.4	17.2	0.99±0.09	71

Condensed Matter and Interphases / Конденсированные среды и межфазные границы   2023;25(3): 435–444

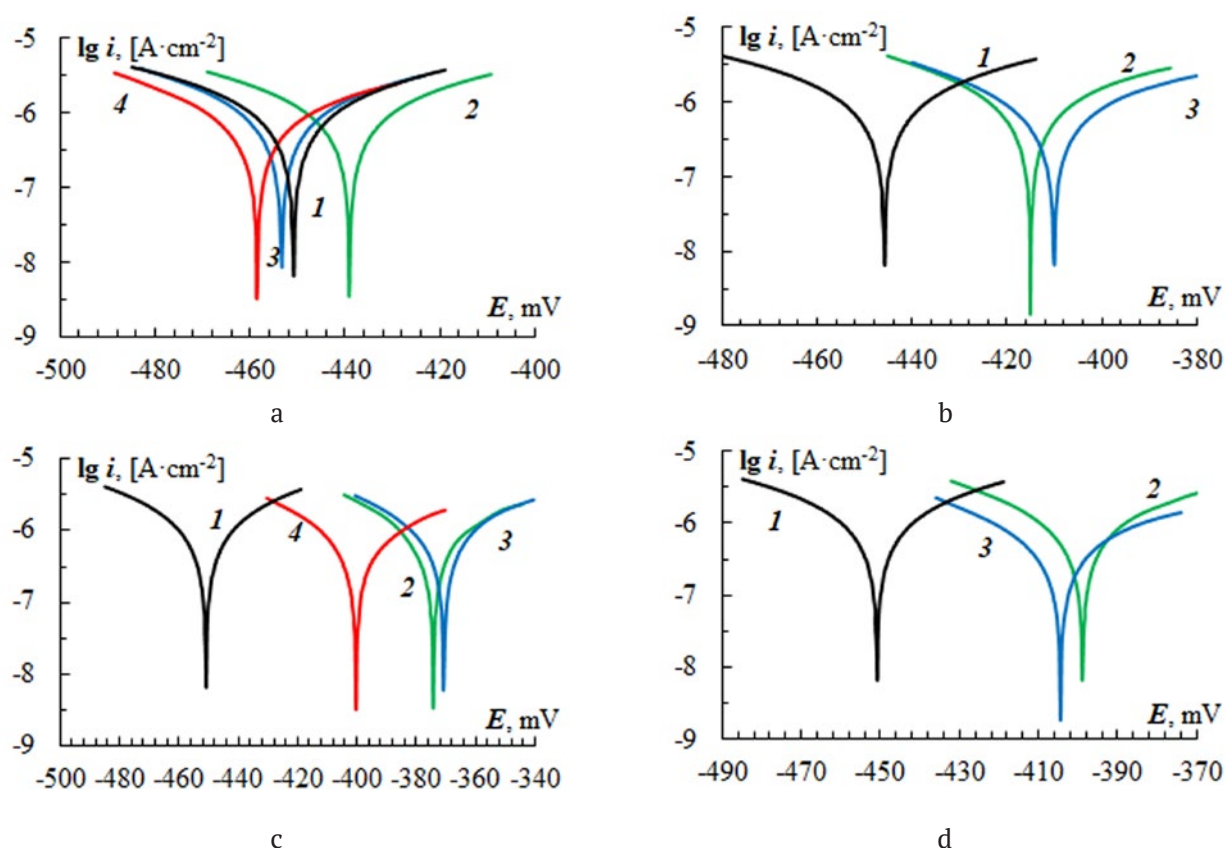O. A. Kozaderov et al.   Inhibitors of chloride corrosion of reinforcement steel in concrete...

Fig. 1. Anodic and cathodic polarization curves of mild steel in water extract from cement + 1.00 mol·dm⁻³ NaCl without an inhibitor (*1*) and in presence of 3-(dimethylamino)propyl-1-ammonium acetate (*a*), 3-(dimethyl-amino)propyl-1-ammonium hexanoate (*b*), 3-(dimethylamino)propyl-1-ammonium octanoate (*c*) and 3-(dime-thylamino)propyl-1-ammonium terephthalate (*d*) a at concentrations of 0.5 (*2*), 1.0 (*3*) and 2.0 g·dm⁻³ (*4*)

46%. Substance *d* is the most effective inhibitor based on the corrosion current density estimated by the method of linear polarization resistance (71% at C_{inh} = 2.0 g·dm⁻³).

3.2. Electrochemical impedance spectroscopy

Nyquist diagrams obtained in reference experiments and in the presence of the studied substances have the same shape of a distorted semicircle with changing diameter and a linear section in the low-frequency region (Fig. 2).

An equivalent circuit presented in Fig. 3 provides a satisfactory description of the diagrams. The results of the calculations are shown in Table 3.

For substances *a*-*b* when the length of the alkyl radical increased form C1 to C5 the degree of protection grew from 9.4 to 19.9% at C_{inh} = 1.0 g·dm⁻³. When the length of the alkyl radical was further increased to C7 with C_{inh} ranging from 0.5 to 1.0 g·dm⁻³, the inhibitory effect was not registered. However, when

C_{inh} = 2.0 g·dm⁻³ the degree of protection was over 35%. For substance *d* the concentration did not affect the degree of protection. Z_i approaches 20%.

3.3. Quantum-chemical calculations

Minimum difference between HOMO and LUMO energies and absolute hardness was observed for compound *d* (Table 4). Compounds *a*-*c* are characterised by higher values of these parameters. Obviously, for *d,* softness is maximum. Therefore, it can be expected to have high adsorption ability and inhibitory properties. *a*-*c* are most likely to have a mild inhibitory effect.

Fig. 4 demonstrates a comparison of the dependencies of inhibitory activity criteria for the studied substances at maximum concentrations. The degree of protection assessed using the polarization resistance method and softness assessed using quantum chemical calculations change symbatically. The inhibition effectiveness assessed using EIS is generally lower than that
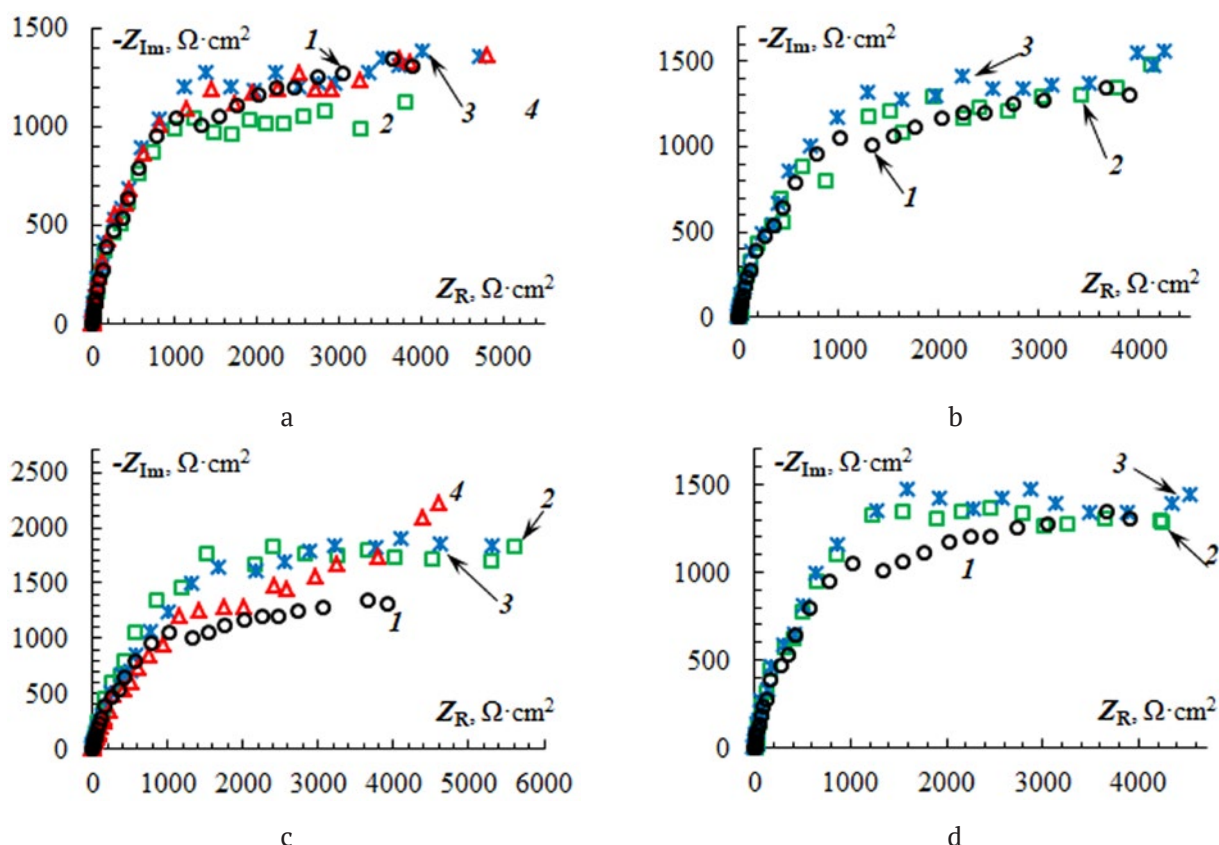
Condensed Matter and Interphases / Конденсированные среды и межфазные границы 2023;25(3): 435–444

O. A. Kozaderov et al. Inhibitors of chloride corrosion of reinforcement steel in concrete...

Fig. 2. Nyquist diagrams of mild steel in water extract from cement + 1.00 mol·dm⁻³ NaCl without an inhibitor (*1*) and in presence of 3-(dimethylamino)propyl-1-ammonium acetate (*a*), 3-(dimethylamino)propyl-1-ammonium hexanoate (*b*), 3-(dimethylamino)propyl-1-ammonium octanoate (*c*) and 3-(dimethylamino)propyl-1-ammonium terephthalate (*d*) a at concentrations of 0.5 (*2*), 1.0 (*3*) and 2.0 g·dm⁻³ (*4*)

Table 3. Calculated equivalent circuit elements of mild steel electrode in water extract from cement + 1.00 mol·dm⁻³ NaCl in presence of derivatives of dimethylaminopropylamine

| Inhibitor	C_{inh}, g·dm⁻³	Equivalent circuit element					η_{inh}, %
		R_Ω, Ω·cm²	R_p, Ω·cm²	CPE_T, μF·cm⁻²	CPE_Φ	BW, Ω·cm²·s⁻⁰·⁵	
blank	–	5.0±0.7	2.9±0.3	9.3±1.2	0.79±0.04	523±55	–
a	0.5	7.8±2.5	3.1±0.3	9.0±0.9	0.77±0.01	510±58	5.3
	1.0	5.4±0.5	3.22±0.11	8.2±0.3	0.80±0.02	601±77	9.4
	2.0	5.6±0.5	3.3±1.2	8.6±0.6	0.77±0.02	442±45	13.7
b	0.5	5.6±0.9	3.2±0.3	9.1±1.3	0.77±0.03	496±57	7.5
	1.0	5.8±0.8	3.6±0.3	9.0±0.7	0.79±0.02	514±47	19.9
c	0.5	6.7±0.6	2.5±0.2	13.6±1.9	0.74±0.01	498±52	−14.6
	1.0	14.7±2.2	2.63±0.6	9.8±0.5	0.76±0.02	789±66	−10.7
	2.0	8.7±1.2	4.5±0.7	10.9±1.1	0.65±0.05	752±74	35.6
d	0.5	6.6±1.5	3.6±0.3	8.3±0.5	0.79±0.03	493±34	19.8
	1.0	5.0±0.1	3.6±0.4	7.9±0.9	0.79±0.03	507±42	19.6
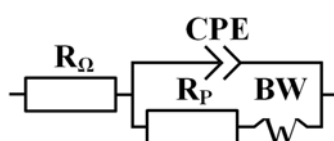
Fig. 3. Equivalent circuit for analysis of electrochemical impedance spectra

Table 4. Calculated energies of HOMO, LUMO, HOMO LUMO gap (HLG), Ionization Potential (IP), Electron Affinity (EA), Absolute Hardness (η) and Softness (σ) in eV at B3LYP/6-311+ G (d, p) level

Inhibitor	E_{HOMO}, eV	E_{LUMO}, eV	HLG, eV	IP, eV	EA, eV	η, eV	σ, eV^{-1}
a	−6.1264	−0,1137	6.0126	6.1264	0.1137	3.0063	0.3326
b	−6.1233	−0.4133	5.7100	6.1233	0.4133	2.8550	0.3502
c	−6.1209	−0.1037	6.0173	6.1209	0.1037	3.0086	0.3324
d	−6.1290	−1.8460	4.2830	6.1290	1.8460	2.1415	0.4669
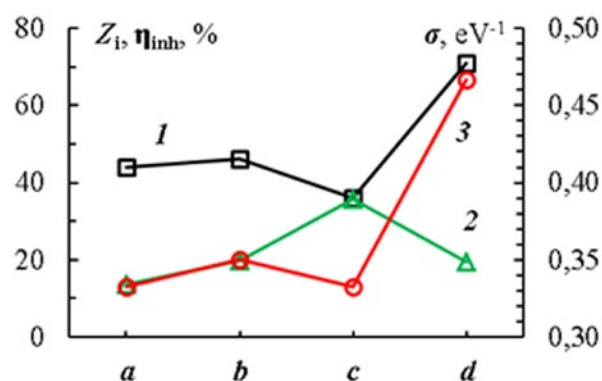
Fig. 4. Degree of protection Z_i (*1*), effectiveness of inhibition η_{inh} (*2*) at the maximum of the studied concentrations and softness σ (*3*) for 3-(dimethylamino)propyl-1-ammonium acetate (***a***), 3-(dimethylamino)propyl-1-ammonium hexanoate (***b***), 3-(dimethylamino)propyl-1-ammonium octanoate (***c***) and 3-(dimethylamino)propyl-1-ammonium terephthalate (***d***)

assessed using PR, but the overall tendency for ***a-c*** remains the same.

The studied substances, when used at maximum concentrations (1.0–2.0 g·dm^{-3}), can be generally characterised as inhibitors with a mild degree of protection. However, we should note that all the experiments were conducted in model liquid environments with a high concentration of chlorides C_{Cl} = 1.00 mol·dm^{-3}. We assume that the studied substances, when used during the production of concrete, can have additional effect on the rheological properties of solutions and physical and mechanical characteristics of set concrete. Lower permeability slows down the penetration of aggressive substances through the concrete shell of reinforcement bars, which can enhance the protective properties. The next stage of this study will include experiments with actual samples of fine-grained concrete.

4. Conclusions

In our study, we synthesised and confirmed the structure of derivatives of salts of carboxylic acids and dimethylaminopropylamine: 3-(dimethylamino)propyl-1-ammonium acetate, 3-(dimethylamino)propyl-1-ammonium hexanoate, 3-(dimethylamino)propyl-1-ammonium octanoate, and 3-(dimethylamino)propyl-1-ammonium terephthalate.

Electrochemical and quantum chemical methods were used to assess the ability of the synthesised compounds to inhibit corrosion of reinforcement steel in a solution simulating concrete pore solution in the presence of chlorides. The results of the polarization measurements, impedance spectroscopy, and quantum chemical calculations are in good agreement. 3-(dimethylamino)propyl-1-ammonium terephthalate is expected to have the highest degree of protection (up to 71%) at the concentration of 2.0 g·dm^{-3}. The highest degree of protection for the derivatives with alkyl radicals is 41–46% in the range of concentrations from 0.5 to 2.0 g·dm^{-3}.

Contribution of the authors

The authors contributed equally to this article.

Conflict of interests

The authors state that they have no known financial conflicts of interest or personal relationships that could affect the work presented in this article.

References

1. Karapetov E. S., Shestovitskiy D. A. Forecast of reinforced concrete bridges' service life on the basis of protective cover carbonization process model. *Proceedings of Petersburg Transport University*. 2016;1: 14–24. (in Russ., abstract in Eng.). Available at: https://www.elibrary.ru/item.asp?id=25776212

2. Samples L. M., Ramirez J. A. *Methods of corrosion protection and durability of concrete bridge decks reinforced with epoxy-coated bars – Phase I*. FHWA/IN/JTPR-98/15 Final Report – West Lafayette. Indiana: Purdue University; 1999. 258 p. https://doi.org/10.5703/1288284313268

Condensed Matter and Interphases / Конденсированные среды и межфазные границы   2023;25(3): 435–444

O. A. Kozaderov et al.   Inhibitors of chloride corrosion of reinforcement steel in concrete…

3. Morgan D. R. Compatibility of concrete repair materials and systems. *Construction and Building Materials*. 1996;10(1): 57–67. https://doi.org/10.1016/0950-0618(95)00060-7

4. Kulinkovich E. D., Nasir M. O. Improving the efficiency of repair-technical service of production by using the concept of total productive maintenance. In: *Research and development in the field of mechanical engineering, energy and management: materials of the XVIII International Scientific and Technical conf. of students, postgraduates and young scientists*. Gomel: 2018. p. 406–409. (in Belarus).

5. Osterminski K. *Zur voll-probabilistischen Modellierung der Korrosion von Stahl in Beton: Ein Beitrag zur Dauerhaftigkeitsbemessung von Stahlbetonbauteilen*: Diss. … Dr.-Ing., München, 2013. 211 p. Available at: https://mediatum.ub.tum.de/doc/1164926/1164926.pdf

6. Falikman V. R., Rozentahl N. K., Stepanova V. F. New Russian norms and codes on protection of building structures against corrosion. In: *High Tech Concrete: Where Technology and Engineering Meet: Proceedings of the 2017 fib Symposium, held in Maastricht*. Netherlands: 2017. pp. 2135–2143. https://doi.org/10.1007/978-3-319-59471-2_244

7. Drochytka R., Ledl M., Bydzovsky J., Zizkova N., Bester J. Use of secondary crystallization and fly ash in waterproofing materials to increase concrete resistance to aggressive gases and liquids. *Advances in Civil Engineering*. 2019; 1–12. https://doi.org/10.1155/2019/7530325

8. Møller V. B., Dam-Johansen K., Frankær S. M., Kiil S. Acid-resistant organic coatings for the chemical industry: a review. *Journal of Coatings Technology and Research*. 2017;14(2): 279-306. https://doi.org/10.1007/s11998-016-9905-2

9. Sharma R., Jang J. G., Bansal P. P. A comprehensive review on effects of mineral admixtures and fibers on engineering properties of ultra-high-performance concrete. *Journal of Building Engineering*. 2022;45: 103314. https://doi.org/10.1016/j.jobe.2021.103314

10. Ban C. C., Khalaf M. A., Ramli M., … Ameri F. Modern heavyweight concrete shielding: Principles, industrial applications and future challenges; review. *Journal of Building Engineering*. 2021;39: 102290. https://doi.org/10.1016/j.jobe.2021.102290

11. Fedrizzi L., Azzolini F., Bonora P. L. The use of migrating corrosion inhibitors to repair motorways' concrete structures contaminated by chlorides. *Cement and Concrete Research*. 2005;35(3): 551–561. https://doi.org/10.1016/j.cemconres.2004.05.018

12. Shevtsov D. S., Zartsyn I. D., … Kozaderov O. A. Evaluation of the efficiency of the Master Life CI 222 organic corrosion inhibitor additive for the protection of steel reinforcement bars in concrete. *International Journal of Corrosion and Scale Inhibition*. 2022;11(4): 1583–1592. https://dx.doi.org/10.17675/2305-6894-2022-11-4-10

13. Gonzalez J. A., Otero E., Feliu S., López W. Initial steps of corrosion in the steel/Ca(OH)$_2$ + Cl– system: the role of heterogeneities on the steel surface and oxygen supply. *Cement and Concrete Research*. 1993;23(1): 33–40. https://doi.org/10.1016/0008-8846(93)90132-S

14. Xu Y., He L., Yang L., Wang X., Huang Y. Electrochemical study of steel corrosion in saturated calcium hydroxide solution with chloride ions and sulfate ions. *Corrosion*. 2018;74(10): 1063–1082. https://doi.org/10.5006/2634

15. Vedalakshmi R., Manoharan S. P., Song H. W. Application of harmonic analysis in measuring the corrosion rate of rebar in concrete. *Corrosion Science*. 2009;51(11): 2777–2789. http://dx.doi.org/10.1016/j.corsci.2009.07.014

16. Bertolini L., Bolzoni F., Gastaldi M. Effects of cathodic prevention on the chloride threshold for steel corrosion in concrete. *Electrochimica Acta*. 2009;54(5): 1452–1463. https://doi.org/10.1016/j.electacta.2008.09.033

17. Schieß P., Mayer T. F., Osterminski K. Influence of the chromate content in cement on the corrosion behaviour of steel in concrete. *Materials and Corrosion*. 2008;59(2): 115–121. https://doi.org/10.1002/maco.200804160

18. Yohai L., Vázquez M., Valcarce M. B. Phosphate ions as corrosion inhibitors for reinforcement steel in chloride-rich environments. *Electrochimica Acta*. 2013;102: 88–96. https://doi.org/10.1016/j.electacta.2013.03.180

19. Ormellese M., Lazzari L., Goidanich S., Fumagalli G., Brenna A. A study of organic substances as inhibitors for chloride-induced corrosion in concrete. *Corrosion Science*. 2009;51(12): 2959–2968. https://doi.org/10.1016/j.corsci.2009.08.018

20. Sagoe-Crentsil K. K., Yilmaz V. T., Glasser F. P. Corrosion inhibition of steel in concrete by carboxylic acids. *Cement and Concrete Research*. 1993;23(6): 1380–1388. https://doi.org/10.1016/0008-8846(93)90075-K

21. Genescaa J., Mendozab J., Duranb R. Conventional DC electrochemical techniques in corrosion testing. In: *XV International Corrosion Congress Manuscript submitted for publication, Metallurgical Engineering*. Mexico: 2002. 17 p.

22. Andreev N. N., Starovoitova E. V., Lebedeva N. A. Inhibition of steel corrosion by benzoic acid salts in calcium hydroxide solutions[*]. *Korrozia: materialy, zashchita*. 2007;5: 29–31. (in Russ.). Available at: https://www.elibrary.ru/item.asp?edn=hexspe

23. Gedvillo I. A., Zhmakina A. S., Andreev N. N., Vesely S. S. Effect of hydroquinone and pyrocatechin on the corrosion and electrochemical behavior of steel

Condensed Matter and Interphases / Конденсированные среды и межфазные границы   2023;25(3): 435–444

O. A. Kozaderov et al.   Inhibitors of chloride corrosion of reinforcement steel in concrete...

in a model concrete pore liquid. *International Journal of Corrosion and Scale Inhibition.* 2019;8(3): 560–572. https://doi.org/10.17675/2305-6894-2019-8-3-7

24. Holmes N., O'Brien R., Basheer P. A. M. Engineering performance of a new siloxane-based corrosion inhibitor. *Materials and Structures.* 2014;47(9): 1531–1543. https://doi.org/10.1617/s11527-013-0133-2

25. Zomorodian A., Behnood A. Review of corrosion inhibitors in reinforced concrete: conventional and green materials. *Buildings.* 2023;13(5); 1170. https://doi.org/10.3390/buildings13051170

26. Raja P. B., Ghoreishiamiri S., Ismail M. Natural corrosion inhibitors for steel reinforcement in concrete – a review. *Surface Review and Letters.* 2015;22(3): 1550040. https://doi.org/10.1142/S0218625X15500407

27. Andreev N. N., Gedvillo I. A., Bulgakov D. S., Zhmakina A. S., Vesely S. S. On penetration of IFKhAN-80 migrating corrosion inhibitor into cement stone. *International Journal of Corrosion and Scale Inhibition.* 2014;3(4): 238–245. http://dx.doi.org/10.17675/2305-6894-2014-3-4-238-245

28. Gedvillo I. A., Zhmakina A. S., Andreev N. N., Vesely S. S. Protection of rusted reinforcing steel in concrete by IFKhAN-85 inhibitor. *International Journal of Corrosion and Scale Inhibition.* 2020;9(2): 562–570. https://doi.org/10.17675/2305-6894-2020-9-2-11

29. Bolzoni F., Brenna A., Ormellese M. Recent advances in the use of inhibitors to prevent chloride-induced corrosion in reinforced concrete. *Cement and Concrete Research.* 2022;154: 106719. https://doi.org/10.1016/j.cemconres.2022.106719

30. Mansfeld F. Tafel slopes and corrosion rates obtained in the pre-Tafel region of polarization curves. *Corrosion Science.* 2005;47(12): 3178–3186. https://doi.org/10.1016/j.corsci.2005.04.012

31. Nam N. D., Van Hien P., Hoai N. T., Thu V. T. H. A study on the mixed corrosion inhibitor with a dominant cathodic inhibitor for mild steel in aqueous chloride solution. *Journal of the Taiwan Institute of Chemical Engineers.* 2018;91: 556–569. https://doi.org/10.1016/j.jtice.2018.06.007

Information about the authors

Oleg A. Kozaderov, Dr. Sci. (Chem.), Docent, Head of the Department of Physical Chemistry, Voronezh State University (Voronezh, Russian Federation).
https://orcid.org/0000-0002-0249-9517
ok@chem.vsu.ru

Dmitry S. Shevtsov, Researcher of the Department of Physical Chemistry, Voronezh State University (Voronezh, Russian Federation).
https://orcid.org/0000-0003-4480-787X
shevtsov@chem.vsu.ru

Mikhail A. Potapov, Researcher of the Department of Physical Chemistry, Voronezh State University (Voronezh, Russian Federation).
https://orcid.org/0000-0002-1795-7605
amidines@mail.ru

Iliya D., Zartsyn, Dr. Sci. (Chem.), Professor of the Department of Physical Chemistry, Voronezh State University (Voronezh, Russian Federation).
https://orcid.org/0000-0002-7161-9754
zar-vrn@mail.ru

Svetlana N. Grushevskaya, Cand. Sci. (Chem.), Docent of the Department of Physical Chemistry, Voronezh State University (Voronezh, Russian Federation).
https://orcid.org/0000-0002-7083-1438
sg@chem.vsu.ru

Alexey A. Kruzhilin, Cand. Sci. (Chem.), Researcher of the Laboratory of Organic Additives for the Processes of Chemical and Electrochemical Deposition of Metals and Alloys Used in the Electronics Industry, Voronezh State University (Voronezh, Russian Federation).
https://orcid.org/0000-0003-2262-0131
kruzhilin.alexey@gmail.com

Evgeniia A. Ilina, Graduate Student of the Department of Physical Chemistry, Voronezh State University (Voronezh, Russian Federation).
https://orcid.org/0009-0004-4825-5894
zhenya.ali@yandex.ru

Kirill A. Tkachenko, Student of the Department of Physical Chemistry, Voronezh State University (Voronezh, Russian Federation).
https://orcid.org/0009-0002-4971-8921
bioshinf1912@mail.ru

Khidmet S. Shikhaliev, Dr. Sci. (Chem.), Professor, Head of the Department of Organic Chemistry, Voronezh State University (Voronezh, Russian Federation).
https://orcid.org/0000-0002-6576-0305
shikh1961@yandex.ru